RESULTS AND DISCUSSION

In order to get physical insight of the problem we have studied the velocity, temperature and concentration against various parameters such as magnetic parameter M, the velocity slip parameter δ, thermal slip parameter β, mass slip parameter ς, Schmidt number Sc and Soret number Sr. The effect of flow parameters on velocity field, skin-friction, Nusselt number and Shearwood number are calculated numerically and discussed with the help of graphs.

We have shown the velocity, temperature and concentration of various values of permeability parameter k* through figures (2)-(4) for vanishing magnetic field. It can be seen from these figures increase in permeability causes an increase in velocity, decrease in temperature and concentration profiles for both slip and no-slip conditions. These results are in good agreement with Asim Aziz *et al.* [3].

Figures (5)-(7) depict the influence of magnetic field M on the velocity, temperature and concentration profiles for both slip and no-slip conditions. We observe that the velocity $f'(\eta)$ along the plate increases when magnetic field increases. Consequently temperature $\theta(\eta)$ and concentration $\phi(\eta)$ decrease when magnetic field increases for both slip and no-slip conditions.

Figures (8)-(10) show the variation in shear stress $f''(\eta)$, the rate of heat and mass transfer for several values of magnetic parameter M. We observe that the increase in magnetic parameter M causes increase in shear stress $f''(\eta)$ and decrease in the rate of heat and mass transfer.

Figures (11)-(16) explain about the effect of slip parameter δ on the velocity, temperature and concentration profiles, shear stress, and the rate of heat and mass transfer. It can be inferred from these graphs that increase in velocity slip parameter δ results in the enhancement of velocity and the rate of mass transfer while, the shear stress, temperature, concentration and the rate of heat transfer decrease due to the increase of slip parameter δ.

Figures (17) and (18) represent the effect of slip parameter β on temperature and the rate of heat transfer. We can observe from these graphs that the increase in slip parameter β results in decrease in temperature and increase in rate of heat transfer.

Figures (19) and (20) show the effect of slip parameter ς on concentration and the rate of mass transfer. We can observe that the increase in slip parameter ς results in decrease in concentration and increase in rate of mass transfer.

Figures (21)-(23) depict that the variation in velocity, temperature and concentration profiles for different values of suction/blowing parameter S. Here, $S>0$ shows the suction and $S<0$ shows the blowing. When suction increases, i.e., $S>0$, fluid velocity increases, which in turn decreases both the fluid boundary layer and the thickness of

momentum boundary layer. Due to suction of the fluid particles at the porous wall, velocity profile increases. In the case of blowing S<0, the opposite trend is observed. When suction increases i.e., S>0, fluid particles come close to the porous wall, due to this temperature profile decreases, which in turn decreases the thermal boundary layer. When suction is increased i.e., S>0, the mass concentration decreases. An opposite phenomena is observed for blowing.

Figures (24) and (25) explain the effect of Schmidt number (Sc) and Soret number(Sr) on concentration profiles. These two figures illustrate that the increase in Schmidt number and Soret number causes decrease and increase in concentration profiles for both slip and no-slip conditions respectively.

Figures (26) and (27) illustrate the effect of Schmidt number (Sc) and Soret number(Sr) on the rate of mass transfer. These two figures illustrate that the increase in Schmidt number and Soret number causes the decrease and increase in $\phi'(0)$ for both slip and no-slip conditions respectively.

Figure (28) explains the effect of skin-friction coefficient $f''(0)$ as a function of the slip parameter δ for various values of magnetic parameter M. It is clear that skin-friction decreases rapidly and approaches zero as the slip parameter δ increases.

Figures (29) and (30) show the rate of heat transfer $\theta'(0)$ as a function of the slip parameters δ and β for various values of magnetic parameter M. We can observe that increase in slip parameters δ and β causes decrease and increase in the rate of heat transfer $\theta'(0)$ respectively.

Figures (31)-(33) exhibit the rate of mass transfer $\phi'(0)$ as a function of the slip parameters δ, β, and ς for various values of magnetic parameter M. We can observe that the rate of mass transfer $\phi'(0)$ decreases, as there is increase in slip parameter δ and β and magnetic parameter M respectively. We can also observe that the rate of mass transfer $\phi'(0)$ increases, with increase in slip parameter ς.

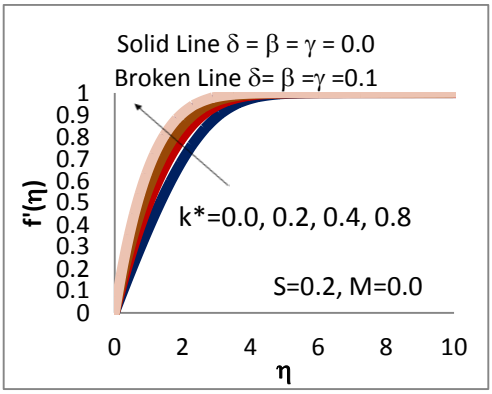

Figure 2. Velocity $f'(\eta)$ for various values of k* under the slip and no-slip boundary conditions.

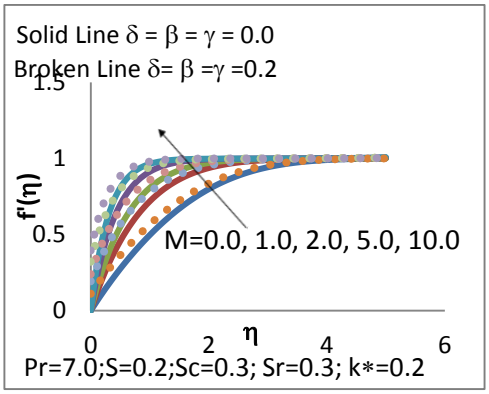

Figure 5. Velocity $f'(\eta)$ for various values of M under the slip and no-slip boundary conditions.

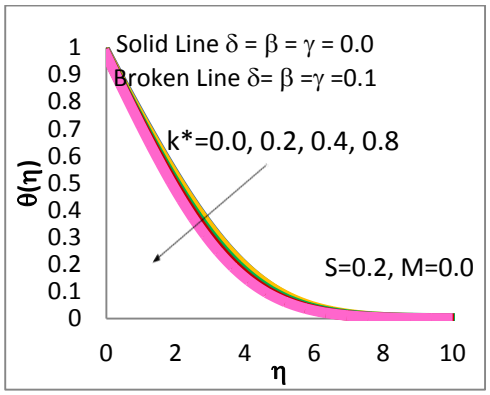

Figure 3. Temperature θ(η) for various values of k* under the slip and no-slip boundary conditions.

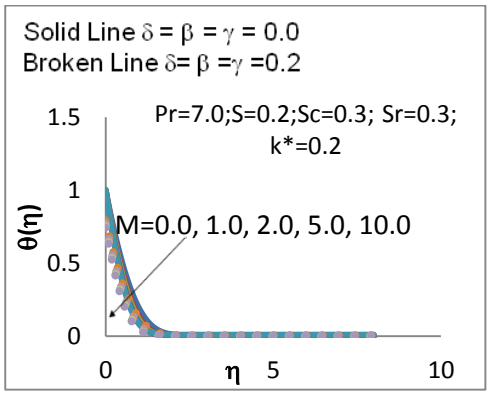

Figure 6. Temperatureθ(η) for various values of M under the slip and no-slip boundary conditions

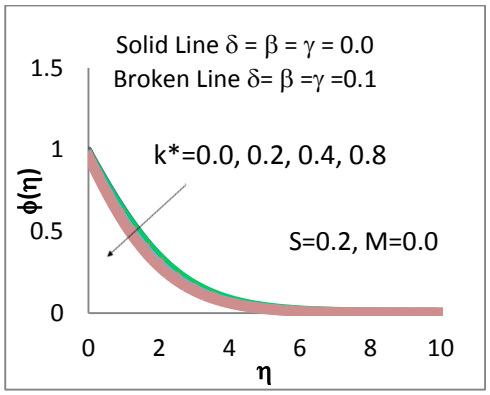

Figure 4. Concentration ϕ(η) for various values of k* under the slip and no-slip boundary conditions.

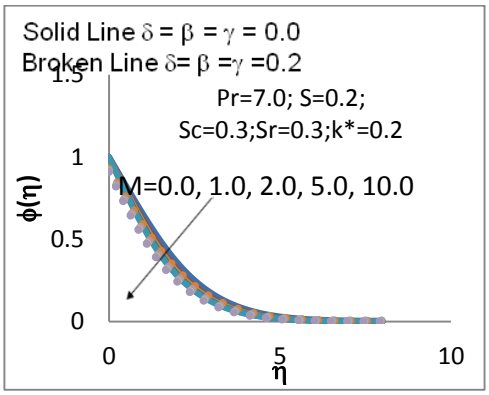

Figure 7. Concentration ϕ(η) for various values of M under the slip and no-slip boundary conditions.

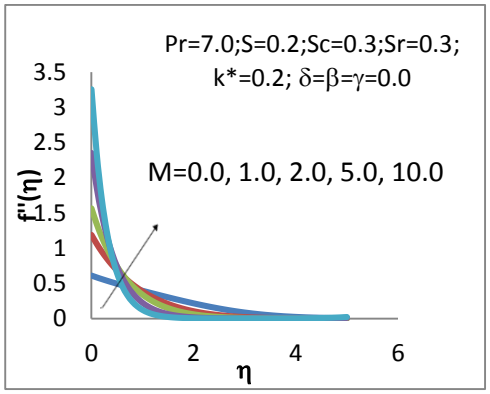

Figure 8. Shear stress profiles $f''(\eta)$ for various values of magnetic field M.

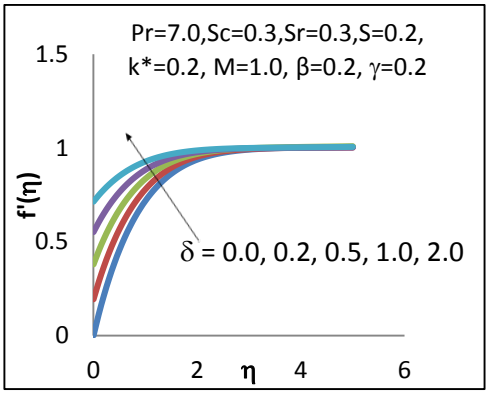

Figure 11. Velocity $f'(\eta)$ for various values of slip parameter δ

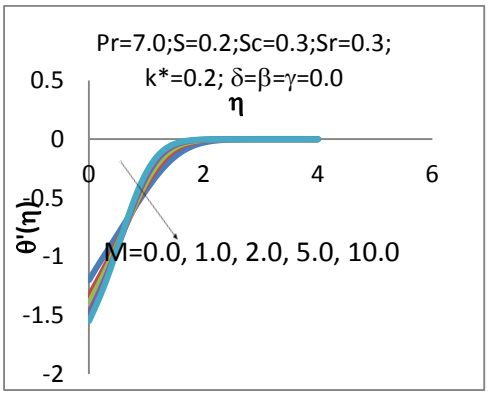

Figure 9. Rate of heat transfer $\theta'(\eta)$ for various values of magnetic field M.

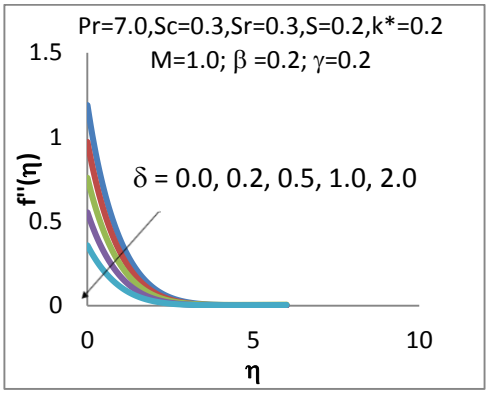

Figure 12. Shear stress $f''(\eta)$ for various values of slip parameter δ

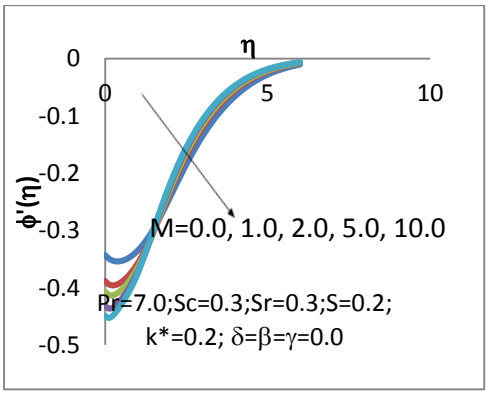

Figure 10. Rate of mass transfer $\phi'(\eta)$ for various values of magnetic field M.

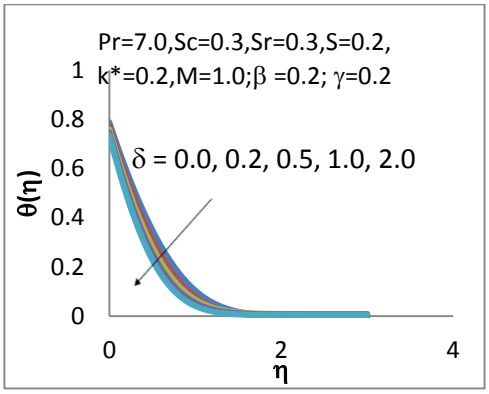

Figure 13. Temperature $\theta(\eta)$ for various values of slip parameter δ.

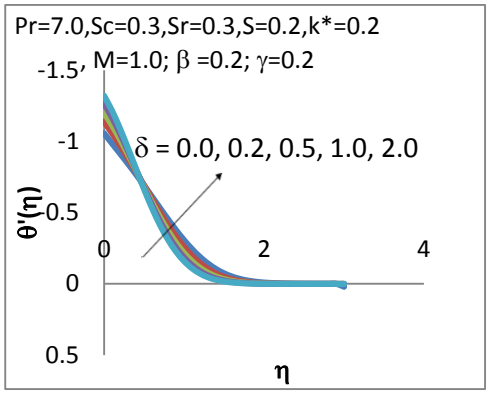

Figure 14. Rate of heat transfer $\theta'(\eta)$ for various values of slip parameter δ.

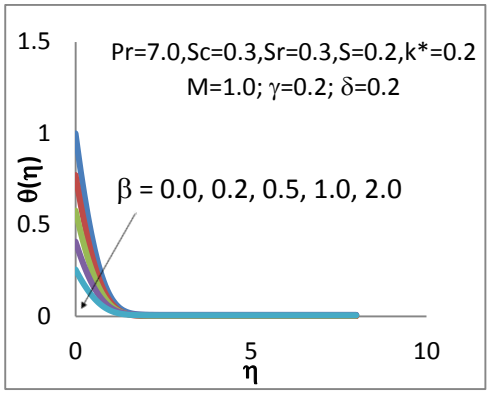

Figure 17. Temperature $\theta(\eta)$ for various values of slip parameter β.

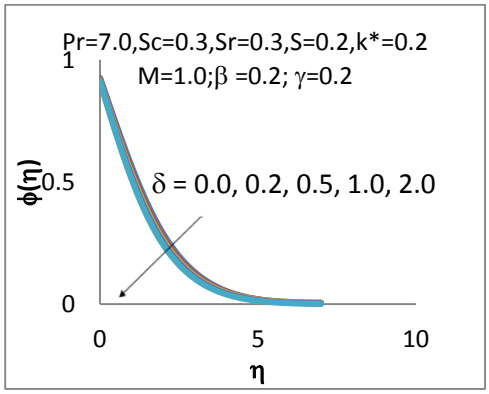

Figure 15. Concentration $\phi(\eta)$ for various values of slip parameter δ.

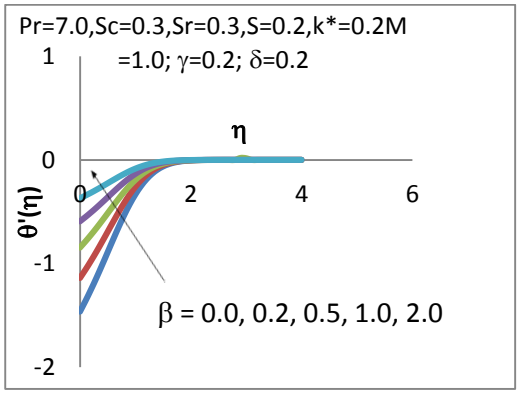

Figure 18. Rate of heat transfer $\theta'(\eta)$ for various values of slip parameter β.

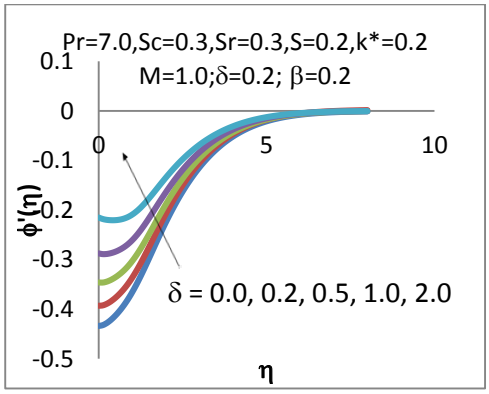

Figure 16. Rate of mass transfer $\phi'(\eta)$ for various values of slip parameter δ.

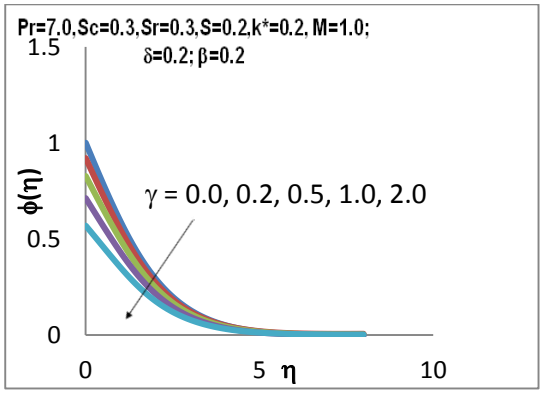

Figure 19. Concentration $\phi(\eta)$ for various values of slip parameter ς

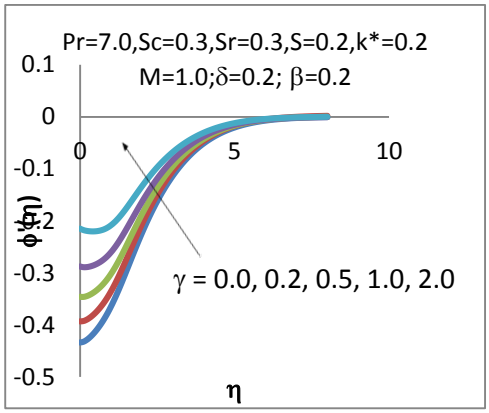

Figure 20. Rate of mass transfer $\phi'(\eta)$ for various values of slip parameter ς

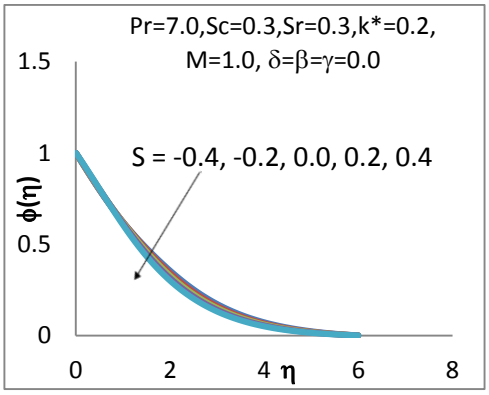

Figure 23. Concentration $\phi(\eta)$ for various values of suction/blowing parameter S

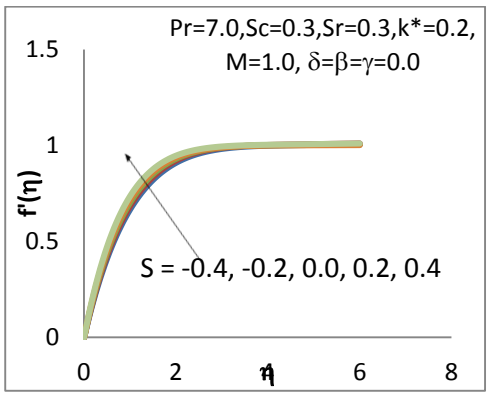

Figure 21. Velocity $f'(\eta)$ for various values of suction / blowing parameter S

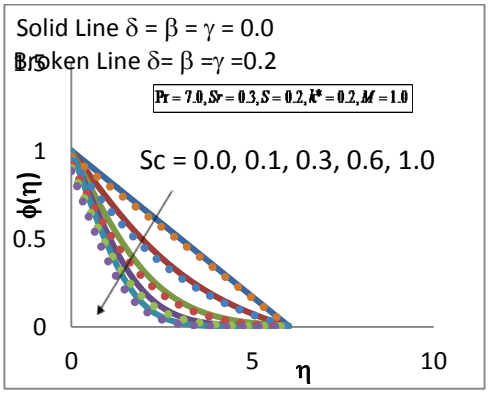

Figure 24. Concentration $\phi(\eta)$ for various values of Sc under the slip and no-slip boundary conditions

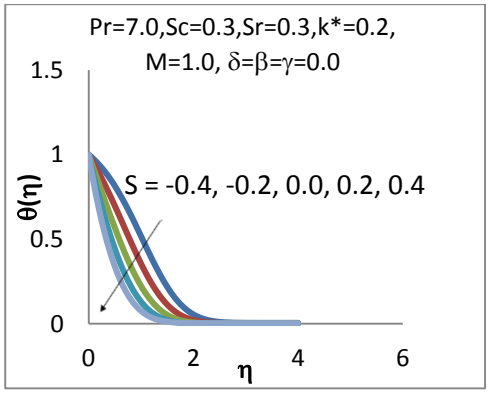

Figure 22. Temperature $\theta(\eta)$ for various values of suction/blowing parameter S

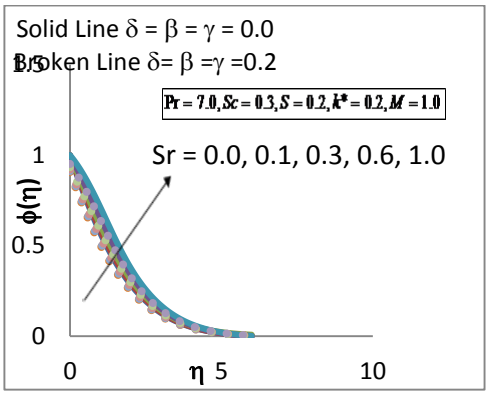

Figure 25. Concentration $\phi(\eta)$ for various values of Sr under the slip and no-slip boundary conditions

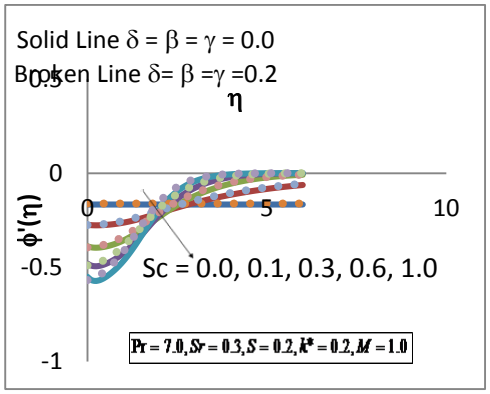

Figure 26. Rate of mass transfer $\phi'(\eta)$ for various values of Sc under the slip and no-slip boundary conditions

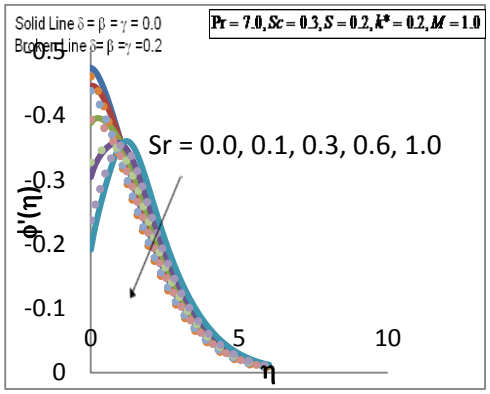

Figure 27. Rate of mass transfer $\phi'(\eta)$ for various values of Sr under the slip and no-slip boundary conditions

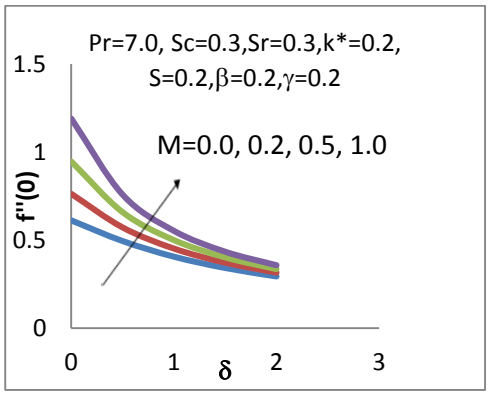

Figure 28. Skin-friction coefficient $f''(0)$ against δ for various values of M

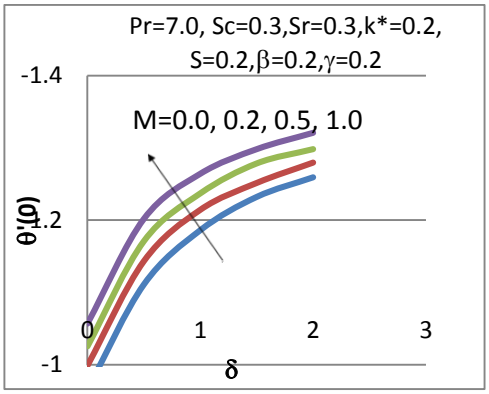

Figure 29. Rate of heat transfer $\theta'(0)$ against δ for various values of M

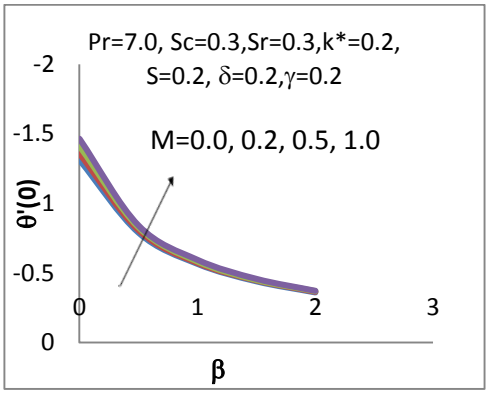

Figure 30. Rate of heat transfer $\theta'(0)$ against β for various values of M

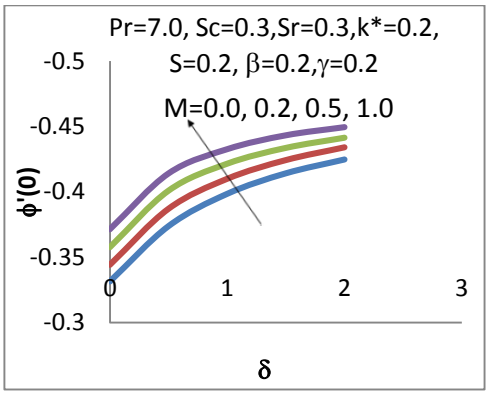

Figure 31. Rate of mass transfer $\phi'(0)$ against δ for various values of M

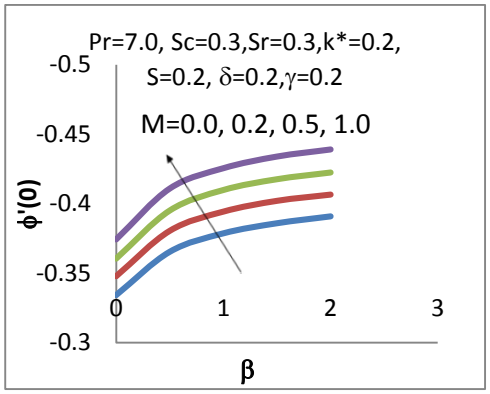

Figure 32. Rate of mass transfer $\phi'(0)$ against β for various values of M

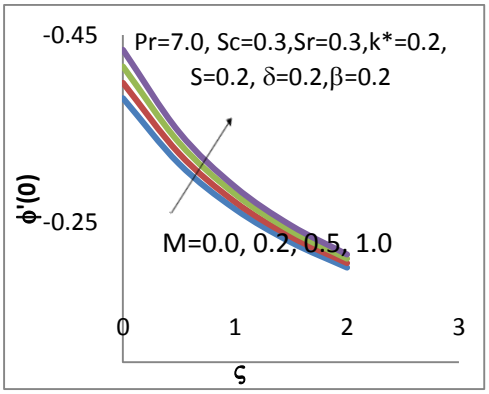

Figure 33. Rate of mass transfer $\phi'(0)$ against ς for various values of M.

CONCLUSION

The effect of MHD convective boundary layer flow along with heat and mass transfer over a porous plate embedded in a porous medium has been investigated. The similarity transformations are used to transform the governing partial differential equations (PDEs) into a system of nonlinear ordinary differential equations (ODEs). The resulting system of ODEs is then reduced to a system of first order differential equations which are solved by shooting procedure using fourth order Runge-Kutta Method. Effect of various non-dimensional parameters on the fluid flow, heat and mass transfer characteristics are examined.

The following conclusions are drawn from the present study:

- Skin-friction decreases rapidly and approaches zero as the velocity slip parameter δ increases.
- The rate of heat transfer $\theta'(0)$ decreases, with increase in the slip parameter δ and magnetic field M. Rate of heat transfer $\theta'(0)$ increases, with increase in the thermal slip parameter β.
- The rate of mass transfer $\phi'(0)$ decreases, as increase in slip parameter δ, β and magnetic parameter M and is also observed that the rate of mass transfer $\phi'(0)$ increases, with increase in slip parameter ς.

REFERENCES

[1] H.I. Andersson, Slip flow past a stretching surface, *Acta Mechanica*, **158**, 121-125, 2002.

[2] S.P. Anjalidavi and R.Kandasamy, Effects of chemical reaction, heat and mass transfer on MHD flow past a semi infinite plate, *Z Angew Math Mech*, **80**, 697–700, 2000.

[3] Asim Aziz, J.I. Siddique, Taha Aziz, Steady Boundary Layer Slip Flow along with Heat and Mass Transfer over a Flat Porous Plate Embedded in a Porous Medium, *PLoS ONE*, **9**, e114544, 2014.

[4] A. Aziz, A similarity solution for laminar thermal boundary layer over a flat plate with a convective surface boundary condition, *A Commun. Nonlinear Sci. Numer. Simulat*, **14**, 1064-1068, 2009.

[5] N. Freidoonimehr, M. M. Rashidi and B. Jalilpour, MHD stagnation-point flow past a stretching/shrinking sheet in the presence of heat generation/absorption and chemical reaction effects, *J Braz. Soc. Mech. Sci. Eng*, **38**, 1-10, 2015.

[6] K. Gangadhar, N. B. Reddy, and P. K. Kameswaran, Similarity solution of hydro magnetic heat and mass transfer over a vertical plate with convective surface boundary condition and chemical reaction, *International Journal of Nonlinear Science*, **3**, 298–307, 2012.

[7] O. D. Makinde, Similarity solution of hydromagnetic heat and mass transfer aover a vertical plate with a convective surface boundary condition, *International Journal of the Physical Sciences*, **5**, 700-710, 2010.

[8] O.D. Makinde, On MHD heat and mass transfer over a moving vertical plate with a convective surface boundary condition, *Canadian Journal of Chemical Engineering*, **88**, 983–990, 2010.

[9] Mohammad Mehdi Rashidi, Behnam Rostami, Navid Freidoonimehr and Saeid Abbasbandy, Free convective heat and mass transfer for MHD fluid flow over a permeable vertical stretching sheet in the presence of the radiation and buoyancy effects, *Ain Shams Engineering Journal*, **5**, 901–912, 2014.

[10] D. Pal and B. Talukdar, Perturbation Analysis of Unsteady Magnetohydrodynamic Convective Heat and Mass Transfer in a Boundary Layer Slip Flow past a Vertical Permeable Plate with Thermal Radiation Chemical Reaction, *Communications in Nonlinear Science and Numerical Simulation*, **15**,1813–1830, 2010.

[11] Santosh Chaudhary and Pradeep Kumar, MHD Slip Flow past a Shrinking Sheet, *Applied Mathematics*, **4**, 574-581, 2013.

[12] E.M. Sparrow and R.D. Cess, The Effect of Magnetic Field on Free Convection Heat Transfer," International Journal of Heat and Mass Transfer, *International Journal of Heat and Mass Transfer*, **3**, 267-274, 1961.